Cell, Vol. 105, 57–67, April 6, 2001, Copyright ©2001 by Cell Press

sidestep Encodes a Target-Derived Attractant Essential for Motor Axon Guidance in *Drosophila*

Helen Sink,*†§ Edward Jay Rehm,* Lee Richstone,* Yolanda M. Bulls,* and Corey S. Goodman*‡
*Howard Hughes Medical Institute
Department of Molecular and Cell Biology
519 LSA
University of California, Berkeley
Berkeley, California 94720
†Skirball Institute of Biomolecular Medicine
Department of Pharmacology
New York University Medical School
540 First Avenue
New York, New York 10016

Summary

At specific choice points in the periphery, subsets of motor axons defasciculate from other axons in the motor nerves and steer into their muscle target regions. Using a large-scale genetic screen in *Drosophila*, we identified the *sidestep* (*side*) gene as essential for motor axons to leave the motor nerves and enter their muscle targets. *side* encodes a target-derived transmembrane protein (Side) that is a novel member of the immunoglobulin superfamily (IgSF). Side is expressed on embryonic muscles during the period when motor axons leave their nerves and extend onto these muscles. In *side* mutant embryos, motor axons fail to extend onto muscles and instead continue to extend along their motor nerves. Ectopic expression of Side results in extensive and prolonged motor axon contact with inappropriate tissues expressing Side.

Introduction

Neuronal growth cones use a variety of substrates and guidance cues to navigate specific choice points and find their correct targets (e.g., Tessier-Lavigne and Goodman, 1996). Among that diversity of substrates and cues, many axons extend selectively along the surface of other axons to form axon bundles or fascicles, a process called selective fasciculation (e.g., Goodman et al., 1984). Just as selective fasciculation provides a specific highway for axon extension, so too growth cones must inevitably exit these axon pathways and steer into their specific target regions in a process called selective defasciculation. Failure to defasciculate at the right choice point can lead growth cones to continue down the main highway, bypassing their correct targets.

For selective fasciculation, the role of cell adhesion molecules (CAMs) is perhaps best understood. In the chick, CAMs play an important role in determining motor axon fasciculation preferences at the limb plexus (Landmesser et al., 1988). The presence of NCAM and L1 on motor axons enhances their attraction for one another. Decreases in NCAM or L1 levels result in enhanced defasciculation (Landmesser et al., 1988). Fasciclin II (Fas II), a CAM in insects that is related to vertebrate NCAM (Harrelson and Goodman, 1988), also plays a role in selective fasciculation. In *Drosophila*, Fas II is expressed on a subset of embryonic CNS axons, many of which selectively fasciculate in three longitudinal pathways. When Fas II is genetically removed, the axons that normally fasciculate together in these pathways fail to do so (Lin et al., 1994). Fas II is also expressed on motor axons. When the levels of Fas II are transgenically increased, motor axons fail to defasciculate at their choice points and instead continue to extend out to the motor nerves, thus bypassing their targets (Lin and Goodman, 1994). Clearly, CAM levels play a critical role in determining motor axon fasciculation.

What controls the ability of motor axons to selectively leave their motor nerves and enter the muscle target region? We are interested in elucidating the molecular mechanisms that control the selective defasciculation of motor axons. One mechanism is to decrease the relative attractiveness of the motor axons for one another, either by decreasing their adhesion or increasing local repulsion. In *Drosophila*, the *beaten path* (*beat*) gene encodes a secreted IgSF protein (Beat) that is expressed by all motor axons at the time of defasciculation and is essential for this process (Fambrough and Goodman, 1996). Motor axons fail to defasciculate at the appropriate choice points in *beat* mutant embryos. It appears that Beat decreases the attractiveness of motor axons for other motor axons, either by directly decreasing the Fas II–mediated attractiveness or by increasing local repulsion.

A second mechanism that could trigger specific defasciculation in this system would be to increase the attractiveness of an alternative substrate, particularly muscle. We present data here on the analysis of the *Drosophila sidestep* (*side*) gene. *side* encodes a protein (Side) that increases the attractiveness of muscles. Side is normally expressed on muscle surfaces during the appropriate stages. In the absence of Side, motor axons fail to defasciculate, do not enter their muscle target regions, and instead continue to extend along the motor nerves. This results in a lack of innervation for a significant proportion of the somatic musculature. Ectopic expression of Side on embryonic tissues contacted by motor axon growth cones results in continued and extensive contact by motor axon growth cones.

Thus, Side functions as a potent attractant for motor axon growth cones. Side is expressed on the surface of the target and presumably functions as a ligand for an unknown receptor on motor axon growth cones. As a target-derived attractant, Side's role is quite distinct from other molecules previously characterized in *Drosophila* that control aspects of neuromuscular specificity.

‡To whom correspondence should be addressed (e-mail: goodman@uclink4.berkeley.edu).
§Present address: Skirball Institute of Biomolecular Medicine, New York University Medical School, New York, New York 10016

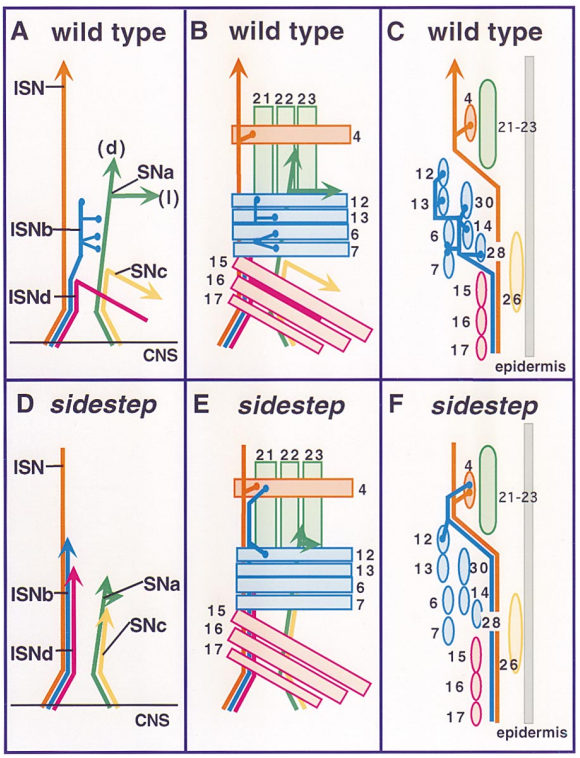

Figure 1. Schematic Diagram of Motor Axons Phenotype in *sidestep* Mutant

Schematic representation of wild type (A, C, and E) and *sidestep* mutant (B, D, and F) motor innervation patterns. In all images, anterior is to the left, and dorsal to the top.

(A) Major branches of the wild-type motor projection in an abdominal hemisegment. ISN, ISNb, and ISNd are the intersegmental major branch, and sub-branches b and d, respectively. SNa and SNc are segmental nerve sub-branches a and c, respectively. ISNb and ISNd are fasciculated with the ISN as they leave the CNS, then defasciculate once in the periphery. SNc is initially fasciculated with the SNa, then also defasciculates in the periphery. Defasciculation takes place at the exit junction.

(B) In wild-type embryos, there is a stereotypic pattern of innervation from each motor projection branch. Each branch innervates correspondingly colored muscles.

(C) Cross-sectional view of wild-type ISNb projection in its target muscle domain.

(D) All branches of the motor projection are perturbed in the *side* mutant. ISNb, ISNd, and SNc fail to defasciculate at the exit junction. Also, the SNa branch that projects to the segment boundary remains fasciculated with the dorsally projecting SNa branch. The ISN is truncated.

(E) In *side* mutant embryos, there is a failure to innervate most of the ventral musculature. There is some correction onto the most distal muscles, such as muscle 12. Axons that fail to correct establish ectopic innervation on more dorsal muscles, such as muscle 4.

(F) In the *side* mutant embryo, the ISNb motor axons fail to defasciculate at muscle 28. Instead, they continue to extend along the ISN.

Results

Motor Axons in *side* Mutant Embryos Fail to Defasciculate at Specific Choice Points

The embryonic *Drosophila* motor projection in the hemisegments of abdominal segments 2–7 consists of 5 major branches (Johansen et al., 1989) (Figures 1A–1C). Each branch of the projection is responsible for innervating a subset (domain) of the 30 stereotypically arrayed muscle fibers (Crossley, 1978; Johansen et al., 1989; Bate, 1990; Van Vactor et al., 1993). The motor projection in a hemisegment is comprised of ~40 motoneurons, each having now been characterized in terms of neuroblast lineage, axon trajectory, and target identity (Halpern et al., 1991; Sink and Whitington, 1991a; Landgraf et al., 1997, Schmid et al., 1999). In addition, there is detailed information on the cellular cues used for guidance by the different motor projection branches (Hartenstein, 1988; Johansen et al., 1989; Sink and Whitington, 1991b; Van Vactor et al., 1993).

The ISN and SNa motor nerves pioneer the foundation of the motor projection. The ISN fasciculates with sensory axons for a portion of its extension in the periphery (Hartenstein, 1988). The motor axons in the ISNb and ISNd branches extend out of the CNS later than the ISN motor axons and fasciculate with the ISN axons during their initial outgrowth into the periphery. Similarly, the motor axons in the SNc branch fasciculate with the SNa axons during their initial outgrowth into the periphery.

At specific locations in the periphery, motor axons defasciculate from other motor axons (or sensory axons) and extend onto muscles. Near the dorsal musculature, the motor axons in the ISN defasciculate from sensory axons and move into the dorsal muscle target domain. At the lateral musculature, motor axons in the SNa defasciculate from one another in order to form the lateral and dorsal branches of the projection. Finally, at the ventral musculature, ISNb and ISNd axons defasciculate from the ISN, and SNc axons defasciculate from the SNa. Once motor axon branches have arrived in their target domain, the motor axons within each branch further defasciculate to attain their final pattern of connectivity with muscle targets (Figures 1A–1C).

In *sidestep* (*side*) mutant embryos, the process of defasciculation is perturbed at these stereotypic locations. Four alleles of *side* were identified in a large-scale chemical mutagenesis screen on the third chromosome on the basis of the motor projection phenotype. A fifth allele was identified in a screen for mutants effecting neuromuscular synapse formation (H. Aberle and C. S. G., unpublished data). While defects occur in all of the motor projection branches in *side* mutant embryos, the severity varies between branches, and in degree of expressivity depending upon the allele (Table 1). For the strongest alleles, the phenotype observed is not enhanced when the alleles are in trans over deficiencies (see $side^{D609}$ allele data in Tables 1 and 2). CNS axon pathways appear wild type, and both neuronal and muscle cell fates appeared normal in *side* embryos when assayed with a panel of antibodies (Van Vactor et al., 1993) (data not shown). These alleles may not be complete nulls, however, since some protein persists (see below).

The ISN in *side* mutant embryos shows three aberrant phenotypes (Figures 2A–2C). These are: (1) failure to reach final branch point in the dorsal muscle domain (TB); (2) failure to innervate muscles despite being in the dorsal muscle domain; and (3) crossing of the anterior segment boundary following contact with the LBD sensory neuron. The SNa (Figure 2C) also exhibits several phenotypes in *side* mutant embryos: (1) failure of either or both the SNa(d) and SNa(l) axons to defasciculate from one another; (2) truncation of either or both

Table 1. Frequency of Defects in Motor Projection Branches in *sidestep* Alleles: Percentage of Hemisegments Where Designated Branch Is Absent

	ISNd	SNc	ISNb M6/7	ISNb M13	ISNb M12	SNa(d)	SNa(L)	FB	SB	TB	ISN X
Control (*red*) (n = 115)	3	0	<1	<1	<1	3	0	0	0	0	0
D282/Df1910 (n = 108)	68	39	88	66	70	13	14	4	4	43	2
H143/Df1910 (n = 88)	89	59	90	75	85	9	13	3	7	43	0
P45/Df1910 (n = 96)	75	58	93	79	93	11	13	1	14	79	3
C137/Df1910 (n = 110)	85	85	86	70	84	3	8	2	6	28	8
D609/Df1910 (n = 112)	88	67	93	80	85	12	6	6	7	39	4

The *side* alleles D282, D609, H143, and P45 were generated in a *red* background. Consequently, *red* is used as the control strain in this analysis. M6/7, M13, and M12 are muscle clefts at which the ISNb arborizes (see Figure 1A). ISN X refers to crossing of the segment boundary by the ISN. Data are presented as % of total hemisegments scored (n) in which the specific branch was absent. The scoring of the phenotype was based only on presence or absence of a branch, not on branch quality.

branches due to an over-fasciculation phenotype; and (3) in rare instances (less than 1% of hemisegments), fasciculation with the ISN. In many hemisegments, the *side* mutant motor projection consists of only the two major motor nerves—the ISN and SNa branches—rather than 5 branches (Figures 1D–1F). This striking phenotype is the result of the failure of ISNb, ISNd, and SNc branches to defasciculate from the ISN and SNa (Figures 2D–2F). Examination of the developing *side* mutant motor projection reveals that these motor axons extend into the periphery and are detectable as large clumps of growth cones tightly associated with the ISN or SNa nerve routes (data not shown). They bypass these muscle targets and extend distally along the ISN and SN.

To follow the fate of individual motor axons that do not defasciculate in the ventral muscle region, we labeled the cell bodies of individual RP motoneurons in the CNS with DiI. In stage 17 wild-type embryos, RP3 motor axons innervate the cleft between muscles 6 and 7 (Figure 3A, n = 10). In contrast, RP3 motor axons in age-matched *side*^{D609} mutant embryos extend along the ISN beyond the ventral muscle region (n = 8). Some of these axons extend well beyond their target's region, exploring the area near dorsal muscle 4 (Figures 3B and 3C, n = 4). Similarly, the RP1 and RP4 neurons, which normally innervate muscle 13 (n = 7), also extended axons along the ISN to locations that ranged from beneath muscle 12 to further dorsally, near muscle 4 (n = 8) (data not shown).

Examination of third instar *side* ^{D609} mutant larval motor projections revealed that the axons normally destined to innervate the ventral musculature had often still failed to correct. As such, ventral muscles such as muscles 6 and 7 remain devoid of innervation (Figure 3F). Interestingly, in hemisegments in which innervation is absent in the ventral muscle domain, hyperinnervation is observed on muscle 4 (Figure 3G). Given the axon tracing data from the embryo, it is likely that this hyperinnervation is from the ISNb and ISNd axons that have failed to target the ventral muscle region.

Cloning of *side* Reveals a Novel Member of the Immunoglobulin Superfamily

Through recombination mapping and deficiency mapping, the cytological location of *side* was narrowed to 98A1-2 on the right arm of the third chromosome, with proximal and distal breakpoints defined by deficiencies Df(3R)Ser^{+R82f} and Df(3R)TI^{5BRXP}, respectively. Our walk (Figure 4A) extended the *pelle* chromosomal walk (Shelton and Wasserman, 1993) a further 120 kb toward the

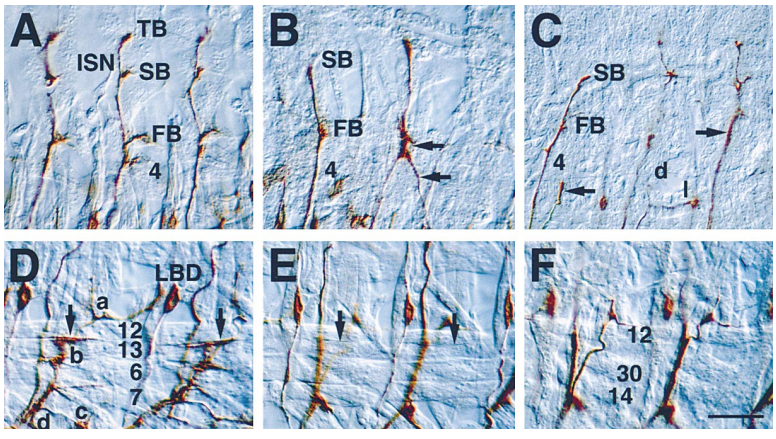

Figure 2. Motor Projection in Wild-type and *side* Mutant Embryos

Embryonic motor projection in stage 17 wild-type (A and D) and *side* mutant (B, C, E, and F) embryos labeled with MAb 1D4.

(A) Wild-type ISN branches in 3 hemisegments. There are three branch points for the ISN: the first (TB), second (SB), and third (FB) branch points.

(B) *side* showing truncation of the ISN at SB in the left hemisegment. The ISN in the middle hemisegment has been joined and fasciculated with by the ISN from the right hemisegment (arrows). This is due to the ISN in the right crossing the segment boundary at the LBD cell.

(C) The ISN in the left hemisegment has failed to extend beyond SB. The SNa in the same segment (arrowhead) has an overly fasciculated SNa(d) but lacks an SNa(l). In the right hemisegment, the SNa has fasciculated with the ISN (arrow).

(D) Wild-type motor projection in the ventral region. a, b, c, and d indicate the SNa, ISNb, SNc, and ISNd branches, respectively, and a subset of muscles innervated by the ISNb are numbered. LBD is the lateral bipolar dendritic neuron, which contributes the sensory component of the transverse nerve. The arrowhead indicates the final branchpoint of the ISNb branch at muscle 12.

(E and F) In *side* mutant embryos, innervation is lacking throughout the ventral musculature (arrowheads in E). Scale bar: 20 μm.

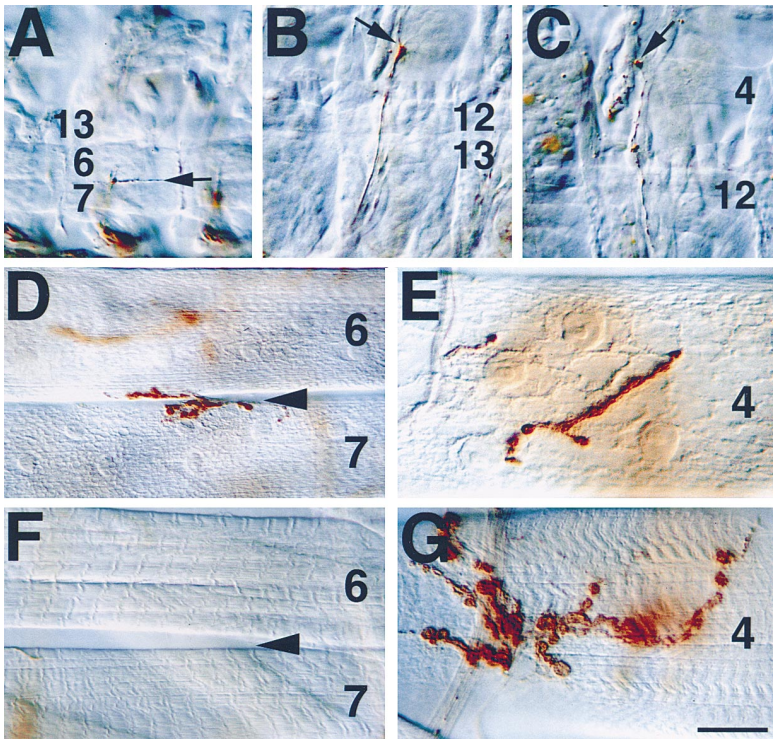

Figure 3. Motor Axon's Arborizations in Wild-type and *side* Mutant Embryos and Larvae

Wild-type embryonic RP3 motor axon arborization (A) at early stage 17 (arrow). In *side* mutant embryos, RP3 axons have extended out to muscle 4 by stage 17 (arrows in B and C). Larval innervation patterns in wild-type (D and F) and *side* mutant larvae (E and G). In wild-type larvae (D), muscles 6 and 7 share innervation along their adjoining cleft (arrowhead). In *side* mutant larvae (F), innervation is absent from the cleft (arrowhead). Muscle 4 receives modest innervation from two branches in wild-type larvae (E). In contrast, *side* mutant larvae show hyperinnervation of muscle 4 (G). Scale bars: 40 μm for (D) and (F) and 30 μm for (A), (B), (C), (E), and (G).

telomere, in the process crossing the distal breakpoints of deficiencies Df(3R)Ser^{+R82f} and Df(3R)TI^{5BRXP} as revealed cytologically with chromosome in situs and molecularly with Southern analysis of RFLPs. Reverse Northern analysis of DNA from our walk uncovered several strongly transcribed regions. A 1.7 kb EcoR1 genomic fragment from one of the regions gave an expression pattern that made it a suitable candidate for being the *side* transcript. Northern analysis with this fragment revealed a single band ~6.5 kb in size. The 1.7 kb EcoR1 fragment was subsequently used to probe an embryonic cDNA library (Zinn et al., 1988). This led to the recovery of 2 cDNAs (8-6 and 4-4) that are ~4 kb in length, and give a stronger, yet identical in situ expression pattern to that of the 1.7 kb EcoR1 fragment.

We sequenced the cDNAs *side* 8-6 and *side* 4-4 on both strands, uncovering a single open reading frame (ORF) encoding a protein (Side) of 864 amino acids (Figure 4B). The Side protein has 5 tandem immunoglobulin-like domains, then a region of almost 200 amino acids with no homology to known domain types. Next is a stretch of hydrophobic amino acids that constitutes a putative transmembrane domain. The relatively short cytoplasmic tail has ~120 aa with no identifiable catalytic domains. An unusual feature of the protein is that the putative signal sequence is distant to the start methionine (Figure 4). To verify that Side is at the cell surface, we expressed *side* in S2 cells. Staining with the anti-Side monoclonal antibody MAb9B8 revealed Side protein on the surface of *side*-transfected cells (Figure 5A) in both the presence and absence of detergent. Side protein was not, however, detected on similarly stained vector-transfected cells (data not shown).

Given the presence of Ig domains on the Side protein, we used the S2 cell aggregation assay to test whether Side could mediate homophilic binding (Elkins et al., 1990). The Side-expressing cells failed to aggregate, and behaved like vector-transfected cells (Figures 5B and 5D). This sharply contrasted with our positive control, S2 cells transfected with Fasciclin II, which gave large cellular aggregates (>100 cells) (Figure 5C).

Drosophila proteins having a 5 Ig domain structure like Side include irregular chiasm-roughest (irreC-rst) (Ramos et al., 1993) and Dumbfounded (Duf) (Ruiz-Gómez et al., 2000). However, the level of conserved amino acid identity between Side and irreC is only 25% for a subset of the Ig domains, while for Side and Duf the proteins are completely divergent at the amino acid level. Closer similarity at the amino acid level is observed between Side and Neuromusculin (Kania et al., 1993). Yet this is also limited to 29% identity, and only for a subset of Ig domains. Searches of available databases did not uncover any homologs of *side*. As such, Side is a novel member of the immunoglobulin superfamily.

We have identified this transcript as that of the *sidestep* gene based on several lines of evidence. First, an antibody against the protein shows that in three mutant alleles (D609, C137, and P45), some protein is evident at later stages, but it is almost undetectable in early embryonic stages. Second, transgenic expression of the *side* cDNA specifically by embryonic muscles largely rescues the mutant phenotype. Third, using the *side* cDNA for RNAi yielded the identical phenotype to the genetic mutant.

Expression of *side* mRNA and Side Protein in the Embryonic CNS

In the CNS at stage 9, the transcript is present in a regularly reiterated pair of cells near the midline that, on the basis of size, shape, and location, are presumably neuroblasts. In stage 10, there are 2–3 strongly positive neuroblasts, and other weaker labeling cells. These cells

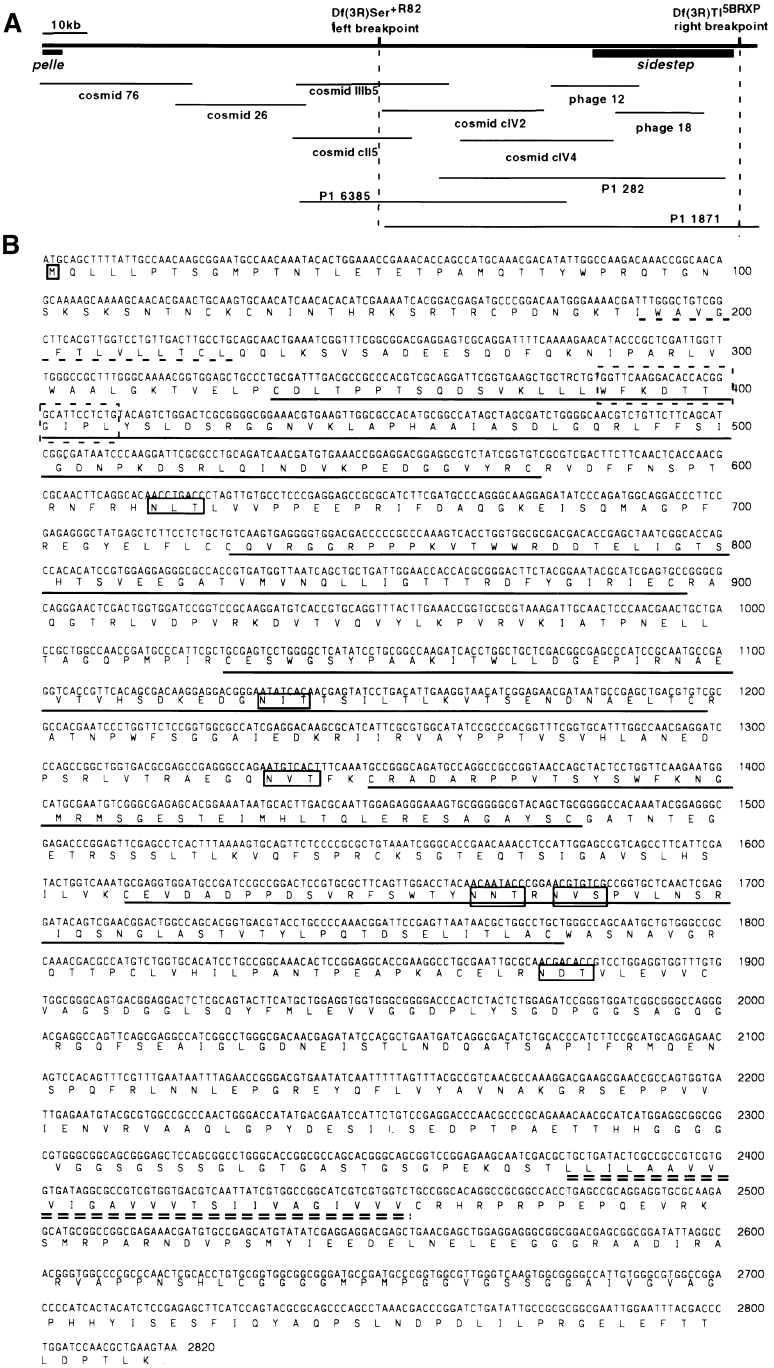

Figure 4. Cloning of the *sidestep* Gene

(A) *sidestep* chromosomal walk. The *sidestep* chromosomal walk continued the *pelle* walk (Shelton and Wasserman, 1993), extending a further 120 kb with phage, cosmid, and P1 steps. Vertical broken lines show left and right breakpoints. The 30 kb area of the walk that contains the *side* transcript is shown as the heavy line in the distal end of the walk.

(B) Nucleotide and deduced amino acid sequence of *sidestep* cDNA 8-6. Highlighted are: the start methionine (bold square); the putative signal sequence (broken underline); the immunoglobulin-like domains between the conserved cysteines (single underline), and the transmembrane region (broken double underline). Potential asparagine-linked glycosylation sites are boxed, and 10 aa in the first Ig domain that are absent in cDNA4.4 are boxed with hatched lines.

divide, giving rise to a number of smaller cells that are also *side*-positive and create a horseshoe shape within each segment. As development proceeds, the number of cells expressing *side* increases.

By stage 13, as axons are extending and forming the commissures and connectives, clusters of cells that lie lateral to the CNS midline express the *side* transcript (Figure 5E). Labeling with MAb 9B8 revealed that in stage 13, Side protein is expressed on subsets of axons in the forming commissural and longitudinal tracts (Figure 5F). During stage 13, Side is also present on the ISN and SN as they extend into the periphery. Neuronal expression decreases during stage 14, with faint labeling from both in situs and immunohistochemistry (Figure 5G). The protein can be detected most strongly at this stage on axons in the longitudinal connectives and the anterior commissure. Neuronal expression increases again in stage 15, so that by the end of embryogenesis in stage 17, the protein is most readily visualized on the longitudinal connectives (Figure 5H).

Expression of *side* mRNA and Side Protein Outside the CNS

In addition to cells within the CNS, *side* is broadly expressed in the periphery. At stage 9, *side* expression in the periphery is evident as 2 patches of cells lying later-

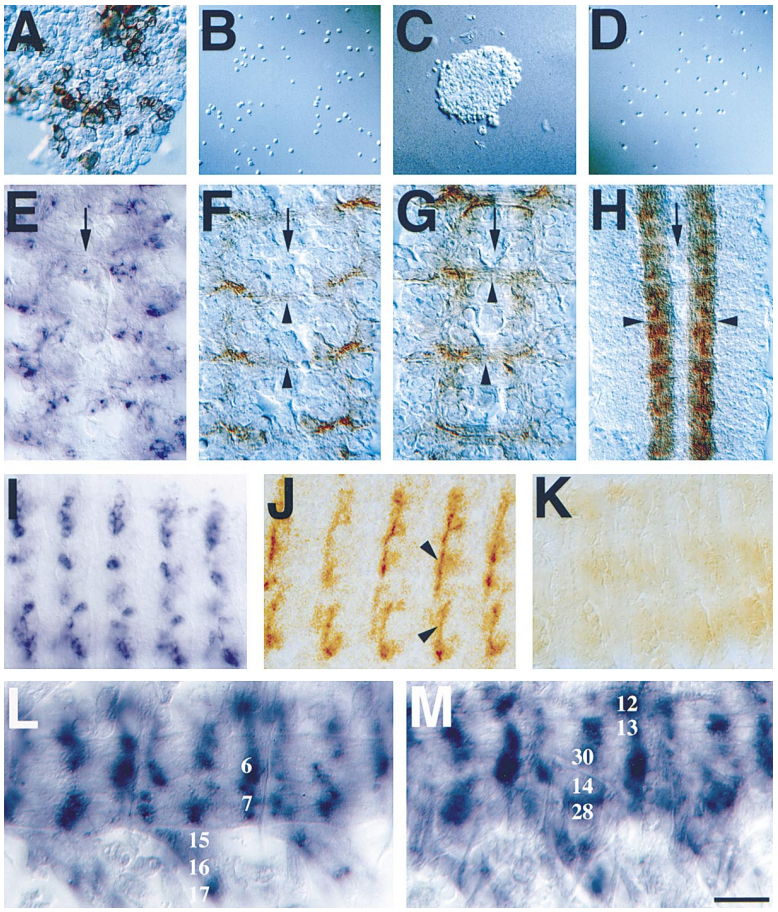

Figure 5. Analysis of *sidestep* Gene and Protein Expression

In transiently tranfected S2 cells, Side protein is detected on the cell surface (A) when stained with MAb9B8 in the absence of detergent (brown cells). Aggregation of S2 cells occurs in cells tranfected with *FasII* (C), but not in cells tranfected with vector (B) or *sidestep* (D). *sidestep* expression in vivo is spatially and temporally highly dynamic. In stage 13 embryos, *side* mRNA (E) is present in a subset of CNS cells lying lateral to the CNS midline (arrow in [E], [F], [G], and [H]). The axons of these cells are extending across the midline (arrowheads in [F]). In stage 17, the Side protein (H) is on many axons in the longitudinal connectives (arrowheads), but barely discernible in the commissures. At stage 14, *side* mRNA is present in a subset of sensory neurons (I), and the axons and cell bodies are expressing Side protein (arrowheads in [J]). In stage 14 $side^{D609}$ embryos, the protein is difficult to detect. (K) *side* is expressed at low levels in the somatic musculature from stage 13 onwards. At stage 16, when the ISNb, ISNd, and SNc are moving into the ventral musculature, *side* is expressed by all of these muscles: (L) shows expression by the internal muscles, while (M) shows expression by the more external muscles. Scale bars: 60 μm for (A); 120 μm for (B–D); 15 μm for (E–G); 25 μm for (H); 50 μm for (I–K); and 20 μm for (L) and (M).

ally and just posterior to the cephalic furrow. During stage 10, two patches of cells lying laterally and anterior to the cephalic furrow become *side*-positive. As segmentation becomes evident at stage 11, *side* transcript is present in a segmentally reiterated cell located dorsally in each hemisegment. Early in stage 12, there are 4 or fewer *side*-positive cells in the dorsal location, and very light levels of transcript in 2 small cell clusters lying midway along the bodywall and closer to the CNS. By stage 13, it appears that these *side*-positive cells are in the sensory neuron clusters present in each hemisegment. During stages 13 and 14, the more dorsally located cells have extended their processes toward the CNS (Figures 5I and 5J), as have those located more ventrally. Side protein is evident on their cell bodies and more strongly on these processes, but is barely detected in our strongest side alleles (Figure 5K). The period of *side* expression by the sensory neurons coincides with when ISN motor axons are extending into the periphery and utilizing sensory axons as guidance substrates. The ISN first contacts the lateral bipolar dendritic (LBD) neuron before moving into contact and fasciculating with axons from the dorsal sensory neuron group (Hartenstein, 1988; Van Vactor et al., 1993). Double labeling with MAb 1D4 and *side* in situs reveals that the ISN motor axons are in contact with a *side*-expressing cell in the LBD group. This site corresponds with the location where the ISN crosses the segment boundary in the *side* mutant. Expression of *side* in the sensory neurons has declined by the end of stage 14.

During stage 13, as muscle fibers are forming, *side* is expressed at high levels in developing somatic muscles. Transcript expression in the dorsal musculature coincides with the arrival of the ISN motor axons in this region. Expression of the *side* mRNA in the somatic musculature decreases, but continues at a low level during stage 15 and into stage 16, when the branches of the ISNb, ISNd, and SNc are defasciculating from the major nerve routes and moving into their target muscle domains (Figures 5L and 5M). During these stages, Side protein is expressed across the surface of all muscles. This expression remains on during stages 16 and 17 in the musculature as synaptogenesis is taking place.

Transgenic Rescue of the *side* Mutant Phenotype

To determine the location of *side* action, we expressed the *side* cDNA 8-6 in muscles or neurons in the $side^{D609}$ background using a *UAS-sidestep* transgene. The *C142-GAL4* line (D. Lin and C. S. G., unpublished data) drives expression in somatic musculature from stage 14 onward. The level of expression in the muscles is somewhat variable between muscles within segments and also for homologous muscles across segments. This is particularly evident in the lateral musculature (Figure 6A). The *elav-GAL4* line (2^{nd} chromosome) drives expression in all postmitotic neurons.

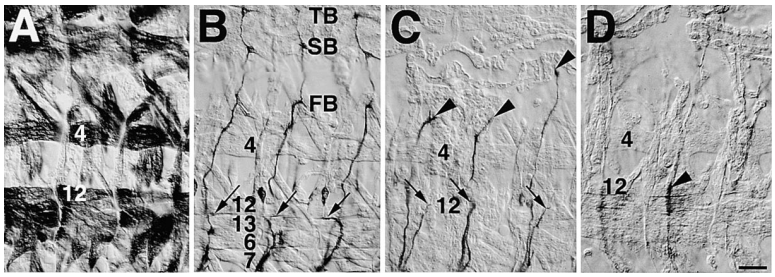

Figure 6. Rescue of *side* Mutant by Transgenic *side* mRNA Muscle Expression

In the *side* mutant background, returning *side* to muscles rescues, whereas expression in the neurons exacerbates the phenotype. The driver *C142;GAL4* was used to return *side* expression to muscles.

(A) Crossing to the reporter line *UAS-lacZ* shows strong β-gal expression in nearly all muscles.

(B) Photomontage of *side*^{D609} embryo with *side* expression returned to muscle. The ISN extends to the final branch point TB, and the ISNb to its final branch point at muscle 12 (arrows).

(C) *side*^{D609} embryo with *sidestep* expressed in all neurons. The ISN halted prematurely in all three segments (arrowheads), as had the SNc (arrows). The ISNb, ISNd, and SNc are absent.

(D) In the *side*^{D609}*/FasII* double mutant, the ventral musculature lacks innervation as assayed with the anti-Late Bloomer MAb. The ISN appears thicker (arrowhead) below muscle 12, suggesting that the ISNb axons are still extending into the periphery along this aberrant route. Scale bar: 20 μm.

Expression of *side* in the musculature resulted in the reversion of most branches of the motor projection toward wild type (Figure 6B, Table 2). Absence of branches was only 26% for the ISNd, 12% for the ISNb, and 20% for ISNc branches, compared to absence levels of 95% for the ISNd, 93% for the ISNb, and 86% for SNc in the *side*^{D609} mutant alone. Similarly, arrival by the ISN at the third branch point was improved from 70% in the mutant, to 93% in the rescue. Given the sensitivity of motor axons to *side* expression levels (see below), the return of *side* expression to the musculature at a higher than normal level yielded a better than expected restoration of the motor projection branching pattern.

Expression of *side* by neurons exacerbated the mutant phenotype, particularly in those branches usually less disrupted in the *side*^{D609} mutant background alone. For the SNa sub-branches, failure to innervate the lateral musculature doubled for the SNa(d) and increased 4-fold for the SNa(l) (Table 2). The result was SNa branches that tended to extend only as far as the area below muscle 12 (Table 2, Figure 6C). Similarly, the ISN stalled earlier and more frequently, with the failure to reach final distal branch point (TB) increasing from 30% in the mutant alone to almost 100% (Table 2, Figure 6C). The ISNb, ISNd, and SNc branches were largely absent (Table 2, Figure 6C). These gain-of-function phenotypes in the loss-of-function background are more severe than those observed for the gain-of-function condition in a wild-type background (see below).

In the *beaten path (beat)* mutant, which has a phenotype that strongly resembles that of the *side* mutant, reduction of the CAM Fas II on axons led to phenotypic rescue (Fambrough and Goodman, 1996). In contrast, when we simultaneously reduced Fas II levels in the *side* mutant background, we did not observe a similar rescue (Figure 6D). Defasciculation by the ISNb axons at muscle 28 was 8.5% in the *side*^{D609} allele (n = 106 hemisegments), and 7.6% in the *side*^{D609}*/Fas II* ^{e76} double mutant (n = 67 hemisegments).

Misexpression of Side Alters Motor Axon Pathfinding and Targeting

We tested the receptiveness of the different projection branches to novel Side contact, either through ectopic presentation or elevated expression levels. Driving expression of *side* in all postmitotic neurons could phenocopy the *side* loss-of-function phenotype. In contrast to the loss-of-function condition, the gain-of-function phenotype was due to the development of the motor projection being greatly delayed. We observed that the ISN was still at the FB choice point at the stage when it would normally be at the final choice point—TB (Figure 7A). Well into stage 16, innervation was also still lacking for much of the ventral musculature, with the ISNb and ISNd absent in each segment and the ISNc greatly reduced (Figure 7C). The neuronal overexpression phenotype seemingly arises through the motor axons behaving as though overly fasciculated. We found that the weaker *elav-GAL4* drivers, such as one on the third chromosome and *C155-GAL4*, do not generate such strong phenotypes. As such, the effect of overexpression of Side in neurons appears to be dosage sensitive. Interestingly, in *UAS-sidestep::elav-GAL4* embryos, the formation of the Fas II-positive longitudinal CNS fascicles remained normal.

In *UAS-sidestep; C38-GAL4* embryos, where *side* is driven throughout the tracheal system, a striking phenotype was observed for the ISN (Figure 7B). During normal

Table 2. Rescue of *sidestep* Phenotypye with a *sidestep* Transgene: Percentage of Hemisegments Where Designated Branch Is Absent

	ISNd	SNc	ISNb M6/7	ISNb M13	ISNb M12	SNa(d)	SNa(L)	FB	SB	TB	ISN X
Control (*red*) (n = 115)	3	0	<1	<1	<1	3	0	0	0	0	0
D609 (n = 125)	95	86	98	93	93	15	17	11	13	30	8
Muscle											
C142:side D609 (n = 112)	26	20	55	12	23	12	11	1	3	7	3
Neuron											
elav:side D609 (n − 112)	96	54	98	99	99	32	70	10	51	97	1

Table format is the same as for Table 1. Scoring of phenotype was based on presence or absence of a branch, not on branch quality.

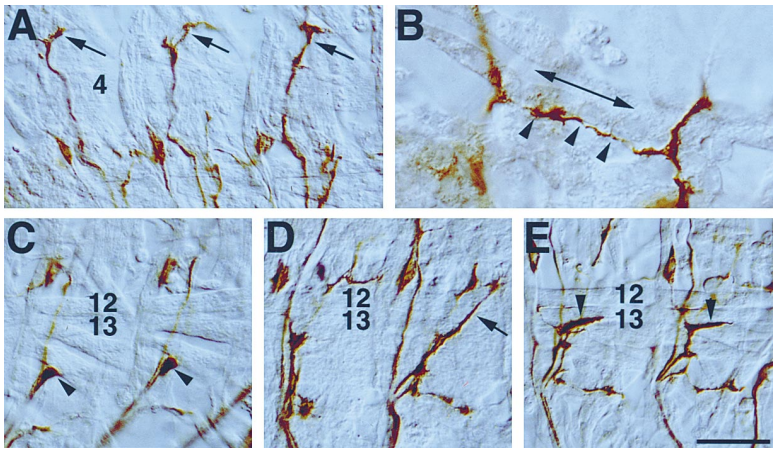

Figure 7. Misexpression and Overexpression of *side*

Misexpression and overexpression of *sidestep* alters motor axon pathfinding and targeting behaviors.

(A) *UAS-side::elav-GAL4/CyO* embryo, where *side* is expressed by all postmitotic neurons, the ISNs have extended only to choice point FB (arrows) although they should be at TB.

(B) Misexpression of *side* in the trachea results in extended contact and exploration by the ISN. Arrowheads indicate aberrant ISN exploration of the main dorsal tracheal trunk. Double-headed arrow is located in the middle of the tracheal trunk.

(C) In a stage 17 *UAS-side::elav-GAL4/CyO* embryo, the ISNb has failed to extend into the ventral musculature (arrowheads), and is still in contact with the ISN and muscle 28. In this *UAS-side::C38-GAL4* embryo (D), the ISNb in one segment is strongly attracted to the Side-expressing tracheole in the region (arrow). When *side* is expressed on muscles 13 and 6, the ISNb axons are strongly drawn to the adjoining surfaces of these two muscles (arrowheads in E). Scale bar: 20 μm for (A), (C), (D), and (E), and 10 μm for (B).

development, the ISN tracks the trachea for a short distance before moving off by fasciculating with incoming sensory axons near the LBD cell (Hartenstein, 1988; Van Vactor et al., 1993). In *UAS-sidestep; C38-GAL4* embryos, the ISN continues tracking the trachea beyond muscle 4 out to the dorsal musculature. In the region of the dorsal musculature, we observe abnormal exploration of the main tracheal trunk by these motor axons (Figure 7B). Similarly, the development of the ISNb can be perturbed by contact with *side*-positive trachea and tracheoles (Figure 7D).

Misexpression of *side* in all of the somatic musculature with the *C142-GAL4* driver did not alter motor axon targeting (data not shown). In contrast, increasing *side* expression in a subset of muscles within a domain with the *H94-GAL4* driver overturned initial targeting preferences. *H94-GAL4* predominantly drives expression in muscles 13 and 6 in the ventral muscle domain (Davis et al., 1997). In *UAS-sidestep; H94-GAL4* embryos, the ISNb axons are strongly attracted to muscle 13 (Figure 7E). By the end of embryogenesis, innervation is present for all muscles in the ventral muscle's domain, although still more exuberant on muscle 13.

Discussion

In this paper we have shown that Side is a potent target-derived attractant of motor axons. Side is a novel member of the immunoglobulin superfamily (IgSF) and is expressed by a variety of cells, including embryonic muscle. In *sidestep* (*side*) mutant embryos, all peripheral branches of the motor projection show varying degrees of the same phenotype: motor axons fail to defasciculate from the major motor nerves. As a result, motor axons fail to enter their muscle target domains and instead continue extending distally along the motor nerves.

The predominant errors occur in the area of the ventral muscle domain just outside the CNS where the motor axons of the ISNb, ISNd, and SNc branches normally defasciculate from the major motor nerves (ISN and SNa). At this choice point, in the absence of Side, these branches do not reliably form because the motor axons fail to defasciculate. Side plays a similar role more distally in guiding ISN and SNa axons onto sensory axons and/or muscle surfaces.

Several studies of the embryonic *Drosophila* neuromuscular system have implicated the mesoderm as providing important cues for ISNb, ISNd, and SNc defasciculation at the ventral choice point. Initial evidence came from examination of *twist* mutant embryos in which mesoderm fails to form. In *twist* mutant embryos, motor axons extend into the periphery, but defasciculation at the ventral choice point fails (Younossi-Hartenstein and Hartenstein, 1993; Prokop et al., 1996). A single muscle founder cell (Bate 1990) can trigger defasciculation of motor axons at this choice point (Landgraf et al., 1999). To date, however, there has been a paucity of information on the nature of the muscle-derived molecular cues that attract motor axons to extend onto muscle surfaces. Our results show that Side is a necessary component of the mesoderm's molecular repertoire for attracting motor axons.

Although analysis of the *side* mutant phenotype shows that variability exists in the requirement for Side to guide different branches, our gain-of-function experiments demonstrate that all branches are highly receptive to the Side signal. Previous misexpression experiments have shown that a diverse range of guidance molecules, including Ig CAMs (Lin and Goodman, 1994; Chiba et al., 1995; Davis et al., 1997), leucine-rich repeat proteins (Nose et al., 1994), Beat (Fambrough and Goodman, 1996), Netrins (Mitchell et al., 1996), Semaphorins (Winberg et al., 1998a; Yu et al., 1998), and Plexins (Winberg et al., 1998b) can alter specific aspects of motor axon pathfinding and targeting. Removal of Side alters all motor axons in a highly penetrant fashion, far stronger than is seen in the absence of any of the previously characterized molecules. Misexpression of Side on virtually any surface in the periphery that is within filopodial grasp of motor axons alters pathfinding, an effect that is further enhanced if the ectopic expression is combined with a *side* mutant. Side appears to function as the major target-derived attractant for all motor ax-

ons, and plays a role that is distinct from other known molecules.

The *side* motor projection closely phenocopies the motor axon behavior observed at the ventral choice point when the relative attractiveness of the motor axons is increased. Overexpression of the Ig CAM Fasciclin II (Fas II) on motor axons enhances axon–axon attraction, and consequently leads to failed defasciculation at the choice point (Lin and Goodman, 1994). Beat is secreted by motor axons, and acts as either a negative regulator of axon–axon attraction or a local repellent. In *beat* mutant embryos, motor axons fail to defasciculate at the ventral choice point (Van Vactor et al., 1993; Fambrough and Goodman, 1996). When Beat is misexpressed on muscles, motor axons avoid the muscles and remain on other axons. Simultaneously decreasing Fas II while removing Beat leads to a partial suppression of the *beat* defasciculation phenotype, and a return of the normal motor branches (Fambrough and Goodman, 1996). In contrast, a reduction in Fas II-mediated axon–axon attraction does not rescue the *side* mutant phenotype. This suggests that the simple reduction in axon–axon attraction cannot compensate for the loss of this potent muscle attractant, further suggesting that Side is a key target-derived attractant in this system. Without its normal expression on muscle, motor axons simply cannot innervate muscle.

General overexpression of Side on all muscle fibers does not result in altered targeting. This is consistent with previous studies that showed that targeting in this system is controlled by a combination of cues on muscle fibers rather than due to a single, highly specific molecular label on each fiber (e.g., Winberg et al., 1998a). An overall increase in the expression of a single molecule on all muscle fibers often results in a more subtle phenotype than changing the differential patterning of the guidance molecule (e.g., Chiba et al., 1995; Matthes et al., 1995; Rose et al., 1997; Winberg et al., 1998b). In line with this model, our general enhancement of attractiveness of the muscles with *side* overexpression did not modify the relative attractiveness within the address system and hence failed to alter targeting. However, when we altered *side* expression levels on a subset of muscles within the ventral muscle domain, targeting preferences were dramatically altered. These observations demonstrate that the presentation of excess Side to motor axon growth cones can override both pathfinding and targeting preferences. However, the condition is temporary. This system has the ability to correct errors over time.

Transgenic expression of Side on all muscles rescues the *side* loss-of-function phenotype. In contrast, transgenic expression of Side on all neurons leads to a defasciculation phenotype similar to the *side* loss-of-function phenotype. Transgenic expression of Side on all neurons in a *side* loss-of-function background exacerbates the loss-of-function phenotype. Our gain-of-function experiments show that all motor axons are highly responsive to Side, indicating that all motor axons possess the molecular machinery necessary to respond to the Side signal. Our in vitro cell aggregation assay and rescue experiments suggest that growth cone responses to Side are unlikely to be attributable to homophilic adhesion. Rather, Side functions as a potent target-derived ligand for an unknown receptor on motor axon growth cones.

The discovery of the *side* gene is a first step toward understanding the nature of muscle-derived signals in this system. What is the Side receptor on motor axon growth cones? Also, given that motor axons defasciculate at specific choice points and enter their muscle target domains, what other muscle-derived cues help control the specificity of these guidance decisions? Further genetic and molecular analysis will hopefully help answer these questions.

Experimental Procedures

Genetic Stocks

Four independent *sidestep* alleles were isolated in a large-scale ethylmethane sulfonate (EMS) mutagenesis screen of over 5000 lines on the third chromosome (H. S. and C. S. G., Soc. Neurosci., abstract, 1994). The additional allele, *sidestep* ^{C137}, was identified in a more recent screen (H. Aberle and C. S. G., unpublished data).

Recombination mapping was carried out against the multiply marked *ru h th st sr e ca* third chromosome. Localization was further refined with deficiencies.

For experiments involving *sidestep* mutant larvae, the *sidestep*^{D609} allele was rebalanced over TM3. For neuron labeling experiments, *side*^{D609} was balanced over a GFP-tagged TM3 balancer and homozygous mutant embryos were identified prior to injection by the absence of GFP. The *sidestep/Fas II* double mutant utilized the *side*^{D609} allele and the *Fas II*^{e76} allele.

Rescue and gain-of-function experiments utilized several GAL4 driver lines. The *MHC*^{82}*-GAL4* line was generated by Margaret Winberg; other GAL4 driver lines used were created by David Lin (Lin and Goodman, 1994).

Cloning of the *sidestep* Gene

The chromosomal walk to the *sidestep* locus was initiated from the distal endpoint of the *pelle* chromosomal walk (Shelton and Wasserman, 1993) using standard techniques, with steps derived from cosmid, phage, and P1 sources. To determine when deficiency breakpoints were crossed, genomic Southerns were made with DNA from deficiency lines and their parental stocks, then probed with walk fragments. Additionally, digoxigenin-labeled DNA probes were prepared from walk fragments and hybridized to polytene chromosomes (BDGP) from Deficiency/Wild type genotype larvae. Two cDNAs (*sidestep* 8-6 and *sidestep* 4-4) were isolated from a 9–12 hr *Drosophila* embryo λgt11 library (Zinn et al., 1988). The sequence of both strands of both cDNAs was obtained using an ALF sequencer (Pharmacia) and a commercial source (Jackson Laboratories), and analyzed with Lasergene software (DNASTAR Inc.).

Generation of Fusion Protein and the Monoclonal Antibody 9B8

A six-histidine-tagged fusion protein was generated by cloning the 1.6 kb Sac1 fragment encoding the Side protein's amino acids 241–786 into the Sac1 site of the pQE30 expression vector (Qiagen). The Sac1 fragment lacks only the first Ig domain of the ectodomain portion of the protein. At 2 week intervals, mice were immunized with 150 μg of fusion protein that had been emulsified in RIBI adjuvent (Immunochem Research). MAb production followed standard procedures.

S2 Cell Aggregation Assays

The cDNA *side*8-6 was completely digested with Sma and partially with EcoR1, and subcloned into RmHa3 vector. S2 cells were transiently transfected using Superfect (Qiagen) in accordance with the manufacturer's directions. Induction of protein expression, assaying of cell aggregation, and immunohistochemistry (with and without saponin detergent) were carried out according to Bieber (1994). As a negative control for aggregation, cells were transfected with RmHa3 vector alone, and as a positive control for aggregation,

S2 cells were transfected with the RmHa3-*Fasciclin II* construct (Fambrough and Goodman, 1996).

RNA Localization, Protein Immunohistochemistry, and Neuronal Labeling

In situ hybridizations were performed with nonradioactive antisense RNA probes as described by Kopczynski et al. (1998). Immunohistochemistry for MAb 1D4 and anti-β-gal staining was performed in accordance with previously described optimized conditions (Van Vactor et al.,1993; Zito et al., 1998). For anti-Side staining, MAb 9B8 was used at a 1:4 dilution. DiI was directly applied to specific RP neuron cell bodies and photo-converted using techniques described in Sink and Whitington (1991a) and Matthes et al. (1995).

sidestep Rescue and *sidestep* Overexpression/ Misexpression

side cDNA 8-6 was subcloned into the EcoR1 site of pUAST (Brand and Perrimon, 1993). Independent transformant lines were obtained on chromosomes X, 2, and 3. Rescue was undertaken using the UAS-GAL4 system. For the neuronal experiment, *UAS-sidestep*^{46} (X chromosome insertion); *sidestep*^{D609}*/TM2*β*-gal* virgin females were crossed to *elav-GAL4/CyO*β*-gal*; *sidestep*^{D609}*/TM2*β*-gal* males. For the rescue experiment where *sidestep* was expressed in muscles, *UAS-sidestep*^{46}*; sidestep*^{D609}*/TM2*β*-gal* virgin females were crossed to *C142-GAL4. C142-GAL4 ; sidestep*^{D609}*/TM2*β*-gal* males.

For overexpression/misexpression experiments, the transformant line *UAS-sidestep*^{46} was crossed to the GAL4 drivers *elav-GAL4/ CyO* (expression in all postmitotic neurons), *C38-GAL4* (expression in trachea), *C142-GAL4* (expression in almost all muscles beginning stage 14), and *H94-GAL4* (expression in a muscle subset).

Acknowledgments

We thank David Van Vactor for assistance in initiating the mutagenesis, and Hermann Aberle for the additional allele. Chris Shelton provided reagents from the *pelle* walk, John Tamkun gave several aliquots of his cosmid library, and Michael Hortsch provided RmHa3 vector DNA. Ron Smith helped generate the *UAS-side* lines. Robert Ramirez and Heather Dworak helped with the S2 cell experiments. Beth Blankemeier helped generate the monoclonal antibody 9B8. H. S. was supported at Berkeley by a postdoctoral fellowship from the Muscular Dystrophy Association and as a Howard Hughes Medical Institute Fellow of the Life Science Research Foundation. At the Skirball Institute, H. S. is funded by NIH grant NS38530. C. S. G. is an Investigator with the Howard Hughes Medical Institute.

Received June 29, 2000; revised February 6, 2001.

References

Bate, M. (1990). The embryonic development of larval muscles in *Drosophila*. Development *110*, 791–804.

Bieber, A.J. (1994). Analysis of cellular adhesion in cultured cells. In Methods in Cell Biology, L.S.B. Goldstein and E.A. Fyrberg, eds. (San Diego: Academic Press).

Brand, A.H., and Perrimon, N. (1993). Targeted gene expression as a means of altering cell fates and generating dominant phenotypes. Development *118*, 401–415.

Chiba, A., Snow, P., Keshishian, H., and Hotta, Y. (1995). Fasciclin III as a synaptic target recognition molecule in *Drosophila*. Nature *374*, 166–168.

Crossley, A.C. (1978). The morphology and development of the *Drosophila* muscular system. In The Genetics and Biology of Drosophila, Vol. 2b, M. Ashburner and T.R.F. Wright, eds. (New York: Academic Press).

Davis, G.W., Schuster, C.M., and Goodman, C.S. (1997). Genetic analysis of the mechanisms controlling target selection: target-derived Fasciclin II regulates the pattern of synapse formation. Neuron *19*, 561–573.

Elkins, T., Hortsch, M., Bieber, A.J., Snow, P.M., and Goodman, C.S. (1990). *Drosophila* fasciclin I is a novel homophilic adhesion molecule that along with fasciclin III can mediate cell sorting. J. Cell Biol. *110*, 1825–1832.

Fambrough, D., and Goodman, C.S. (1996). The *Drosophila* beaten path gene encodes a novel secreted protein that regulates defasciculation at motor axon choice points. Cell *87*, 1049–1058.

Goodman, C.S., Bastiani, M.J., Doe, C.Q., du Lac, S., Helfand, S.L., Kuwada, J.Y., and Thomas, J.B. (1984). Cell recognition during neuronal development. Science *225*, 1271–1279.

Halpern, M.E., Chiba, A., Johansen, J., and Keshishian, H. (1991). Growth cone behavior underlying the development of stereotypic synaptic connections in *Drosophila* embryos. J. Neurosci. *11*, 3227–3238.

Harrelson, A.L., and Goodman, C.S. (1988). Growth cone guidance in insects: Fasciclin II is a member of the immunoglobulin superfamily. Science *242*, 700–708.

Hartenstein, V. (1988). Development of *Drosophila* larval sensory organs: spatiotemporal pattern of sensory neurones, peripheral axon pathways and sensilla differentiation. Development *102*, 869–886.

Johansen, J., Halpern, M.E., and Keshishian, H. (1989). Axonal guidance and the development of muscle fiber-specific innervation in *Drosophila* embryos. J. Neurosci. *9*, 4318–4332.

Kania, A., Han, P.L., Kim, Y.T., and Bellen, H. (1993). Neuromusculin, a *Drosophila* gene expressed in peripheral neuronal precursors and muscles, encodes a cell adhesion molecule. Neuron *11*, 673–687.

Kopczynski, C.C., Noordermeer, J.N., Serano, T.L., Chen, W.Y., Pendleton, J.D., Lewis, S., Goodman, C.S., and Rubin, G.M. (1998). A high throughput screen to identify secreted and transmembrane proteins involved in *Drosophila* embryogenesis. Proc. Natl. Acad. Sci. USA *95*, 9973–9978.

Landgraf, M., Bossing, T., Technau, G.M., and Bate, M. (1997). The origin, location, and projections of the embryonic abdominal motorneurons of *Drosophila*. J. Neurosci. *17*, 9642–9655.

Landgraf, M., Baylies, M., and Bate, M. (1999). Muscle founder cells regulate defasciculation and targeting of motor axons in the *Drosophila* embryo. Curr. Biol. *9*, 589–592.

Landmesser, L., Dahm, L., Schultz, K., and Rutishauser, U. (1988). Distinct roles for adhesion molecules during innervation of embryonic chick muscle. Dev. Biol. *130*, 645–670.

Lin, D.M., and Goodman, C.S. (1994). Ectopic and increased expression of Fasciclin II alters motoneuron growth cone guidance. Neuron. *13*, 507–523.

Lin, D.M., Fetter, R.D., Kopczynski, C., Grenningloh, G., and Goodman, C.S. (1994). Genetic analysis of Fasciclin II in *Drosophila*: defasciculation, refasciculation, and altered fasciculation. Neuron *13*, 1055–1069.

Matthes, D.J., Sink, H., Kolodkin, A.L., and Goodman, C.S. (1995). Semaphorin II can function as a selective inhibitor of specific synaptic arborizations. Cell *81*, 631–639.

Mitchell, K.J., Doyle, J.L., Serafini, T., Kennedy, T.E., Tessier-Lavigne, M., Goodman, C.S., and Dickson, B.J. (1996). Genetic analysis of Netrin genes in *Drosophila*: Netrins guide CNS commissural axons and peripheral motor axons. Neuron *17*, 203–215.

Nose, A., Takeichi, M., and Goodman, C.S. (1994). Ectopic expression of connectin reveals a repulsive function during growth cone guidance and synapse formation. Neuron *13*, 525–539.

Prokop, A., Landgraf, M., Rushton, E., Broadie, K., and Bate, M. (1996). Presynaptic development at the *Drosophila* neuromuscular junction: assembly and localization of presynaptic active zones. Neuron *17*, 617–626.

Ramos, R.G., Igloi, G.L., Lichte, B., Baumann, U., Maier, D., Schneider, T., Brandstatter, J.H., Frohlich, A., and Fischbach, K.F. (1993). The irregular chiasm C-roughest locus of *Drosophila*, which affects axonal projections and programmed cell death, encodes a novel immunoglobulin-like protein. Genes Dev. *7*, 2533–2547.

Rose, D., Zhu, X., Kose, H., Hoang, B., Cho, J., and Chiba, A. (1997). Toll, a muscle cell surface molecule, locally inhibits synaptic initiation of the RP3 motoneuron growth cone in *Drosophila*. Development *124*, 1561–1571.

Ruiz-Gómez, M., Coutts, N., Price, A., Taylor, M.V., and Bate, M. (2000). *Drosophila* Dumbfounded: A myoblast attractant essential for fusion. Cell *102*, 189–198.

Schmid, A., Chiba, A., and Doe, C.Q. (1999). Clonal analysis of *Drosophila* embryonic neuroblasts: neural cell types, axon projections and muscle targets. Development *126*, 4653–4689.

Shelton, C.A., and Wasserman, S.A. (1993). *pelle* encodes a protein kinase required to establish dorsoventral polarity in the *Drosophila* embryo. Cell *72*, 515–525.

Sink, H., and Whitington, P.M. (1991a). Location and connectivity of abdominal motoneurons in the embryo and larva of *Drosophila* melanogaster. J. Neurobiol. *22*, 298–311.

Sink, H., and Whitington, P.M. (1991b). Pathfinding in the central nervous system and periphery by identified embryonic *Drosophila* motor axons. Development *112*, 307–316.

Tessier-Lavigne, M., and Goodman, C.S. (1996). The molecular biology of axon guidance. Science *274*, 1123–1133.

Van Vactor, D., Sink, H., Fambrough, D., Tsoo, R., and Goodman, C.S. (1993). Genes that control neuromuscular specificity in *Drosophila*. Cell *73*, 1137–1153.

Winberg, M.L., Mitchell, K.J., and Goodman, C.S. (1998a). Genetic analysis of the mechanisms controlling target selection: complementary and combinatorial functions of netrins, semaphorins, and IgCAMs. Cell *93*, 581–591.

Winberg, M.L., Noordermeer, J.N., Tamagnone, L., Comoglio, P.M., Spriggs, M.K., Tessier-Lavigne, M., and Goodman, C.S. (1998b). Plexin A is a neuronal semaphorin receptor that controls axon guidance. Cell *95*, 903–916.

Younossi-Hartenstein, A., and Hartenstein, V. (1993). The role of the tracheae and musculature during pathfinding of *Drosophila* embryonic sensory axons. Dev. Biol. *158*, 430–447.

Yu, H.H., Araj, H.H., Ralls, S.A., and Kolodkin, A.L. (1998). The transmembrane Semaphorin Sema I is required in *Drosophila* for embryonic motor and CNS axon guidance. Neuron *20*, 207–220.

Zinn, K., McAllister, L., and Goodman, C.S. (1988). Sequence analysis and neuronal expression of fasciclin I in grasshopper and *Drosophila*. Cell *53*, 577–587.

Zito, K., Fetter, R.D., Goodman, C.S., and Isacoff, E.Y. (1998). Synaptic clustering of Fasciclin II and Shaker: Essential targeting sequences and role of Dlg. Neuron *19*, 1007–1016.

Accession Numbers

The sequence of the *sidestep* gene has been submitted to GenBank with accession number AF358267.